Reprinted (adapted) with permission from The Journal of Physical Chemistry A, *Classical Collision Spectrum of O + CO*, M. Braunstein and J.W. Duff, America Chemical Society, August 10, 2009.

J. Phys. Chem. A **2009,** *113,* 10795–10802

Classical Collision Spectrum of O + CO

M. Braunstein* and J. W. Duff

Spectral Sciences Incorporated, 4 Fourth Avenue, Burlington, Massachusetts 01803

Received: May 1, 2009; Revised Manuscript Received: August 10, 2009

The work of Noid et al. [*J. Chem. Phys.* **1977**, *67*, 404] has shown that sharp molecular spectra can be obtained through a Fourier transform of the autocorrelation function of a classical trajectory. In the present work, we extend this idea to obtain a spectrum by Fourier transform of the dipole moment function of collision product trajectories. We show that this "classical collision spectrum" (CCS) is related to the cross section for creating the product times an Einstein A factor. As a test case, we analyze product CO trajectories obtained from O + CO collisions at 8 km/s and focus on the spectral resolution of the CCS. The CCS of these trajectories shows rich quantum-like features, including well-separated vibrational overtones and rotational band heads, which become more pronounced with particular trajectory weighting methods. For polyatomic cases, the hope is that the CCS can be deconvolved into ro-vibrational specific probabilities and cross sections for quasi-periodic trajectories, which would otherwise overlap in a conventional classical trajectory energy analysis. Chaotic trajectories are expected to broaden and decrease the achievable resolution of the CCS. Chaotic motion will therefore impact the ability to separate ro-vibrational specific cross sections, an issue that will be addressed in future work.

I. Introduction

About thirty years ago, Noid et al. demonstrated how molecular spectra could be obtained from an analysis of classical trajectories.[1] By Fourier transforming a suitable autocorrelation function, they obtained accurate, sharp-featured spectra for several model Hamiltonian systems. More recently, Fourier analysis of the velocity autocorrelation and dipole moment functions of classical trajectories have been used to analyze the dynamics and generate spectra for a wide variety of systems, including CH_5^+ (ref 2) and the hydrated proton.[3] In the present work, we extend the work of Noid et al. to an analysis of spectra of quasi-classical trajectory (QCT) collision products. The goal is to develop improved methods of characterizing the final state collision products in terms of quantum-specific states. For polyatomic products, conventional QCT binning methods have great difficulty in separating ro-vibrational cross section contributions due to overlaps in a particular energy bin. Several methods have been developed to separate and assign ro-vibrational specific motion in classical trajectories. Schatz and co-workers developed methods based on the fast Fourier transform method and determination of good action angle variables through space-fixed and normal mode transformations.[4] Hase and co-workers have also developed methods to quantize vibrational motion for polyatomics by transforming to the Eckart rotating axis frame.[5] In general, these methods have proven difficult to apply to general cases.

The calculation procedure we developed involves first performing QCT calculations of molecular collisions at a particular collision energy, with each trajectory sampling a range of orientation and impact parameters in the usual way.[6] At the end of each trajectory, however, we retain the final positions and momenta of the collided products. Then, using this set of final positions and momenta, we continue each trajectory and Fourier transform the dipole moment of the collided products. The weighted average of these transforms is a "classical collision spectrum" (CCS) of the nascent collision products, which is related to the cross section for creating the product times an Einstein A factor.

The CCS, obtained by straightforward extension of standard QCT methods, may offer several benefits for analysis of classical trajectories. With knowledge of measured or calculated product Einstein *A* values, and if final product spectral contributions do not overlap too much, it may be possible to deconvolve the CCS and estimate quantum specific cross sections. The idea is that ro-vibrational product cross sections, which would otherwise overlap in a conventional internal energy analysis, will separate more cleanly in the classical collision spectrum. The CCS may also be compared directly to molecular beam experiments where spectra of the nascent collision products are measured, providing a useful common point of analysis between experimental observables and theory. Finally, as ab initio molecular dynamics becomes more routinely used, with accurate forces and dipole moments available at each trajectory step, generation of the CCS should be readily achievable, even for very large molecules.

An important potential complication of the CCS method is the possible presence of chaotic motion in classical trajectories, especially if this motion does not have a quantum analog.[7] Quasi-periodic motion leads to well-defined spectral lines. Classically chaotic motion, which may exist even at the zero point level,[8] will effectively broaden the classical spectrum by introducing many weak lines clustered near the expected transition energies.[5,9] In general, at lower energies for polyatomic systems, trajectories are quasi-periodic and smoothly transition to a more chaotic motion with increasing energy. However, particular molecules and motion may not follow this trend, and it is difficult to predict the degree of chaos expected for a particular case. Cho et al.,[10] for example, found the onset of chaos of the bending mode of HCN at ~11 000 cm^{-1}. However, the onset for chaos for the stretching modes was ~26 000 cm^{-1}, and only a fraction of the stretching modes became chaotic below the dissociation threshold. For many systems examined, the classical power spectrum appears to retain discrete band-like features, even at high energies[11] and even where the degree

10.1021/jp904055y CCC: $40.75 © 2009 American Chemical Society
Published on Web 09/16/2009

of classical chaos is judged to be large.[10] In general, chaotic trajectory broadening is expected to decrease the achievable resolution of the CCS. Chaotic motion will therefore impact the ability to separate ro-vibrational specific cross sections, an issue that will be addressed in future work on polyatomic systems. In the present work, we focus on formulation of the method and application to a well-characterized system which gives sharp spectra even at very high energies.

In section II, we develop the theory of the CCS. Starting with the work of Noid et al., we obtain an expression relating the CCS of a single trajectory to a set of Einstein A values and transition energies. We then show that the weighted average of classical spectra can be related to the ro-vibrational specific cross section times a set of Einstein A values. In section III, we illustrate the method by examining $O(^3P) + CO(^1\Sigma_g)$ collisions at 8 km/s. We used the potential energy surfaces and product CO trajectories of our previous QCT studies,[12,13] in which the product state distributions compared well to measurements.[13−15] For the CO diatomic product, conventional QCT methods provide ro-vibrational specific cross sections which serve as a benchmark test case with which to compare the CCS results. We first investigate the dependence of the CCS results on the semiclassical vibrational and rotational actions and on numerical integration errors for single $CO(v,j)$ semiclassical trajectories. We then generate classical spectra of the product CO, averaging over a large set of O + CO trajectories. The resulting CCS of the O + CO collision trajectories shows rich quantum-like features, including well-separated vibrational overtones and rotational band heads, which become more pronounced with particular trajectory weighting methods. In section IV, we give conclusions and discuss possible future applications to polyatomic systems.

II. Methods

In this section we derive an expression relating the Fourier transform of the dipole moment of a single classical trajectory to a set of Einstein A values and transition energies, which we call a classical collision spectrum (CCS). We then show that a weighted average of these CCS is related to the product of a ro-vibrational specific collision cross section times this set of Einstein A values. In principle, these relationships allow the deconvolution of the averaged CCS obtained from trajectories of collision products into ro-vibrational specific cross sections.

Following Noid et al.,[1] we start with the definition of the line-shape function, $I(w)$:

$$I(\omega) = \frac{1}{2\pi}\int_{-\infty}^{\infty} C(t)\mathrm{e}^{-\mathrm{i}\omega t}\,\mathrm{d}t \tag{1}$$

where $C(t) = \langle x(0)\,x(t)\rangle$ is the autocorrelation of some dynamical variable, $x(t)$ (coordinate, dipole moment, etc.), and the brackets denote an ensemble average. Noid et al. show that for an ergodic or quasi-periodic trajectory, the brackets can be removed to yield an expression,

$$I(\omega) = \frac{1}{2\pi}\lim_{T\to\infty}\frac{1}{T}\left|\int_0^T x(t)\mathrm{e}^{-\mathrm{i}\omega t}\,\mathrm{d}t\right|^2 \tag{2}$$

For an absorption line shape, the dynamical variable $x(t) = \vec{\mu}(t)$, where $\vec{\mu}(t)$ is the dipole moment function. We can relate the absorption line shape, $I(\omega)$, to the absorption cross section, $\alpha(\omega)$, of a single trajectory,[16]

$$\alpha(\omega) = \frac{4\pi\omega I(\omega)}{3\hbar c} \tag{3}$$

The integral of the absorption cross section with respect to the frequency near an absorption line center is the absorption coefficient, S, which is related to the Einstein A value,[17]

$$S = \int \alpha(\omega)\,\mathrm{d}\nu = \frac{c^2}{8\pi^2\nu^2}A_{\mathrm{ul}}\frac{g_{\mathrm{u}}}{g_{\mathrm{l}}} \tag{4}$$

In the above equation, A_{ul} is the Einstein A coefficient from an upper state, u, to a lower state, l, and g_{u} and g_{l}, respectively, are the degeneracies of the upper and lower states. We note that the full absorption spectrum will contain a number of lines connecting the lower state l to a set of upper states {u}. Substituting eq 3 into eq 4, and using eq 2 for the absorption line shape, we can relate the Einstein A coefficients to the Fourier transform of the dipole moment function of a single trajectory:

$$A_{\{\mathrm{u}\}\mathrm{l}}(\lambda) = \frac{64\pi^4}{3h\lambda^3}\frac{g_{\mathrm{l}}}{g_{\mathrm{u}}}\int \mathrm{d}\nu\,\frac{1}{T}\left|\int_0^{\infty}\vec{\mu}(t)\mathrm{e}^{-\mathrm{i}\omega t}\,\mathrm{d}t\right|^2 \tag{5}$$

In eq 5, λ is the wavelength, and $A_{\{\mathrm{u}\}\mathrm{l}}(\lambda)$, which we call the classical collision spectrum (CCS), is a set of Einstein A coefficients connecting the lower state l with all dipole allowed upper states {u} at the transition wavelengths $\lambda_{\mathrm{l}\{\mathrm{u}\}} = \{\lambda_{\mathrm{lu1}}, \lambda_{\mathrm{lu2}}, \text{etc.}\}$. In other words, the expression $A_{\{\mathrm{u}\}\mathrm{l}}(\lambda)$ represents a classical analog of an absorption stick spectrum of a particular ro-vibrational state l defined by the initial position and momentum of the trajectory. The peak heights are equal to the Einstein A values from the upper state u to the lower state l, and the wavelengths at which the peaks appear are the transition wavelengths from l to u. Formulating the CCS in this way facilitates comparison to literature values of the Einstein A coefficients. To evaluate eq 5 in practice, we compute a discrete Fourier transform over a time window of length T for each of the vector components of the dipole moment function, and we approximate the integration interval over the frequency, ν, around each line by multiplying each Fourier transform frequency bin by the bin width, $1/T$,

$$\begin{aligned} A_{\{\mathrm{u}\}\mathrm{l}}(\lambda_k) \approx \frac{64\pi^4}{3h\lambda^3}\frac{g_{\mathrm{l}}}{g_{\mathrm{u}}}\frac{1}{T^2}\Big[\Big|\Delta t\sum_{n=1}^{N}\hat{x}\cdot\vec{\mu}(t_n)\mathrm{e}^{-\mathrm{i}2\pi nk/N}\Big|^2 + {} \\ \Big|\Delta t\sum_{n=1}^{N}\hat{y}\cdot\vec{\mu}(t_n)\mathrm{e}^{-\mathrm{i}2\pi nk/N}\Big|^2 + \Big|\Delta t\sum_{n=1}^{N}\hat{z}\cdot\vec{\mu}(t_n)\mathrm{e}^{-\mathrm{i}2\pi nk/N}\Big|^2\Big] \end{aligned} \tag{6}$$

In eq 6, Δt is the discrete Fourier transform time step, $T = N\Delta t$, where N is the number of Fourier transform time steps, $\{\hat{x}, \hat{y}, \hat{z}\}$are unit vectors along the Cartesian $\{x, y, z\}$ directions, n denotes a time bin, and k a frequency bin.

Now suppose a number of molecular trajectory collisions are performed in the standard QCT manner, where an average over the relative orientation of the reagents and over the collision impact parameter is taken in the usual way. For a particular trajectory, once the products are far away from each other, we take the position and momentum of one of the products to define the ro-vibrational state l. Analogous to the expression for the collision cross section, we write the average of the CCS over a number of such trajectories,

$$\bar{A}(\lambda) = \frac{1}{\sum_{1}^{N_{\text{tot}}} w_l} \sum_{1}^{N_{\text{tot}}} w_l A_{\{u\}l} \tag{7}$$

In eq 7, N_{tot} is the total number of trajectories, w_l is the weight of the trajectory with final position and momentum l, and $A_{\{u\}l}$ are CCS of individual trajectories associated with a particular l. In standard QCT, each trajectory has the same statistical weight. The weighting factor, w, in eq 7 follows the work of Rayez and co-workers and others.[18−20] They have shown that weighting semiclassical trajectories with Gaussian-like coefficients centered near integer vibrational actions, which is analogous to choosing integer actions for reagents, builds in quantum-like behavior and leads to improved agreement with corresponding quantum mechanical results. Using standard QCT methods for choosing the initial orientation of reagents and if we bin the l states into quantum specific ro-vibrational product states, q, we can write the probabilities and cross sections in terms of the weights,

$$P_q = \frac{\sum_{l \to q} w_l}{\sum_{1}^{N_{\text{tot}}} w_l} = \frac{\sigma_q}{\sigma_{\text{tot}}} = \frac{\pi b_{\max}{}^2 \sum_{l \to q} w_l}{\pi b_{\max}{}^2 \sum_{1}^{N_{\text{tot}}} w_l} \tag{8}$$

where in eq 8, $\sum_{l \to q} w_l$ represents the sum of all those trajectories, l, binned into ro-vibrational state, q, $b_{\max}$ is the maximum impact parameter of the QCT calculations, σ_q is the cross section to the ro-vibrational product state q, P_q is the probability of forming the products in state q, and σ_{tot} is the sum of all σ_q. We now write eq 7 in terms of the probability of molecular collisions which lead to the ro-vibrational state q,

$$\bar{A}(\lambda) = \sum_{q} P_q A_{\{u\}q} \tag{9}$$

Equations 6−9 are the main results of this section. Equation 9 shows that the averaged CCS, $\bar{A}(\lambda)$, can be interpreted as an absorption spectrum of the nascent products of molecular collisions. These equations also provide an alternative way to estimate the ro-vibrational specific probabilities and cross sections from standard QCT methods. We first generate the CCS average, $\bar{A}(\lambda)$, from eqs 6 and 7. Then with knowledge of the Einstein A coefficients we can deconvolve the spectrum for the quantum specific probabilities P_q using Equation 9. The hope is that the average CCS will separate contributions of different product states, q, which would otherwise overlap in conventional energy binning analysis.

The usefulness of the averaged CCS and the deconvolution procedure will depend on how cleanly the averaged CCS separate into ro-vibrational contributions and in the details of numerical implementation. In the next section we investigate these issues by examining the CCS of single trajectories of the CO molecule and by using various weighting methods to compute averaged CCS for collisions of CO with atomic oxygen.

III. Results

A. Single Trajectories. We now examine CCS of single trajectories of the CO molecule. All results use the potential and QCT methods of refs 12 and 13 and the CO dipole moment function of ref 21. Figure 1 shows four different CCS, each computed with eq 6. Each CCS used different initial positions and momenta, l, labeled by their semiclassical actions, ($v = 0$, $j = 90$), ($v = 1$, $j = 90$), ($v = 2$, $j = 90$), and ($v = 3$, $j = 90$), and prepared using standard WKB methods.[6] The trajectories were integrated with a standard velocity Verlet algorithm,[22] with 10^6 time steps of 1×10^{-16} s spacing. The FFT of each trajectory was obtained by zero-padding the trajectory to the next power of 2, 2^{20} points, giving a spectral bin width of 0.318 cm^{-1}. These parameters are associated with our “standard” numerical convergence parameters. Examining a single trajectory, we observe the expected absorption progression of $\Delta v = 0$, 1, 2, 3 peaks. The $\Delta v = 0$ region contains one transition corresponding to an “absorption” from $j = 90 \rightarrow 91$. The other spectral regions each have “P” and “R” pair peaks associated with a unit change in the rotational “quantum number”. As shown below, the peak positions are all within ~10 cm^{-1} of reference positions for transitions obtained by computing the WKB energies with this same potential. We point out that the WKB energies are not exact for the nonharmonic CO potential used here. The WKB energies and transitions are used as a convenient consistency check. Noid et al. have shown similar good agreement between classical power spectrum peaks and exact quantum mechanical eignvalues.[1] The Einstein A coefficients agree qualitatively with benchmark calculations using a similar quality potential and dipole moment function. It is interesting that several quantum features of the absorption spectrum, including overtones and rotational selection rules, are recovered fairly well by such classical trajectories.

As Noid et al.[1] show, the exact spectral peak locations will depend on the choice of semiclassical quantum number. Figure 2 shows the CCS of CO computed with eq 6 near $\Delta v = 1$ transitions. Five spectra are shown, each with a different classical action for the initial condition $l = (v, j)$. These initial conditions are centered around ($v = 1$, $j = 90$): ($v = 0.5$, $j = 90$), ($v = 0.75$, $j = 90$),($v = 1.0$, $j = 90$), ($v = 1.25$, $j = 90$), and ($v = 1.5$, $j = 90$). As the classical action is varied near a vibrational action of 1.0, the peak positions shift and the peak heights change. To examine this more in depth, Figure 3 shows the transition energy versus error in CCS peak position for 11 different transitions associated with the progression, $v, j = 90 \rightarrow v - 1, j = 89$, where $v = 1 \rightarrow 11$. We chose to analyze this progression in depth because these transitions are prominent in the band-head structure of the emission spectra of 8 km/s O + CO collisions[12−15] and because the results are fairly representative of other transitions we have examined. The reference transition energies are obtained by computing the WKB energies of CO with the same potential with the semiclassical quantum numbers ($v = 1 \rightarrow 11$, $j = 90$) and ($v = 0 \rightarrow 10$, $j = 89$) and taking the difference between the results. The CCS results are obtained with trajectories composed of 10^7 time steps of 10^{-18} s in width. The Fourier transform was obtained by zero-padding the trajectory to the next power 2 making 2^{24} points, giving a spectral bin width of 0.0199 cm^{-1}. These parameters are associated with our “fine” numerical convergence parameters. For averages over many trajectories, fine parameter convergence can become impractical, but for single trajectories they are useful to illustrate the degree of numerical error in practical computation. The error shown in Figure 3 is the CCS peak energy bin value minus the corresponding WKB transition energy. CCS results are shown for 5 different choices of the semiclassical quantum numbers $l = (v, j)$: ($v - 0.5$, $j = 89.5$), ($v - 0.5$, $j = 90$), ($v - 0.5$, $j = 89$), (v, $j = 89.5$), and ($v - 1$, $j = 89.5$). These five choices show the variation in the CCS peak positions

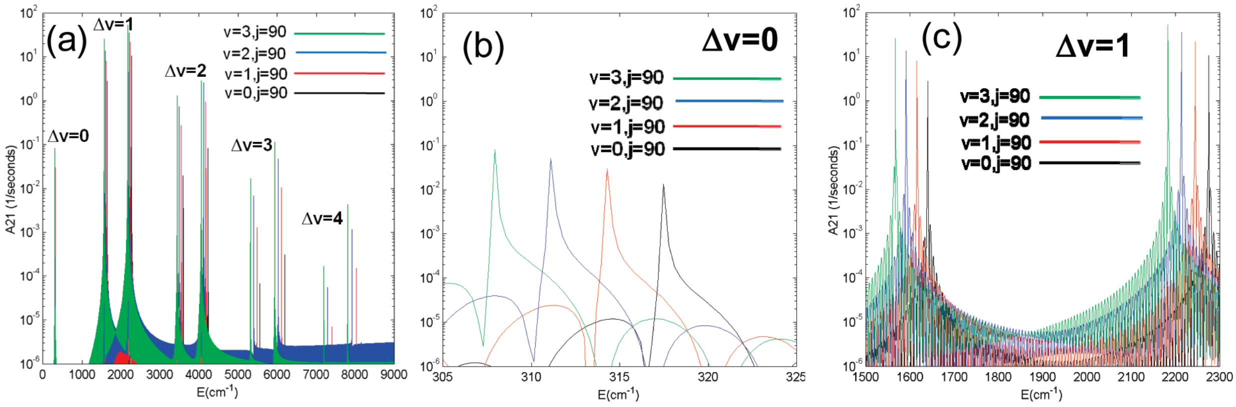

Figure 1. Classical collision spectra (CCS), $A_{\{u\}l}(\lambda)$, of CO computed with eq 6. Four spectra are shown, each with a different classical action $l = (v, j)$: ($v = 0, j = 90$), ($v = 1, j = 90$), ($v = 2, j = 90$), and ($v = 3, j = 90$). (a) CCS over a large energy and intensity scale. The Δv notation suggests the corresponding quantum vibrational state transitions. (b) Same as (a) except the range of $\Delta v = 0$ transitions has been expanded. (c) Same as (a) except the range of $\Delta v = 1$ transitions has been expanded.

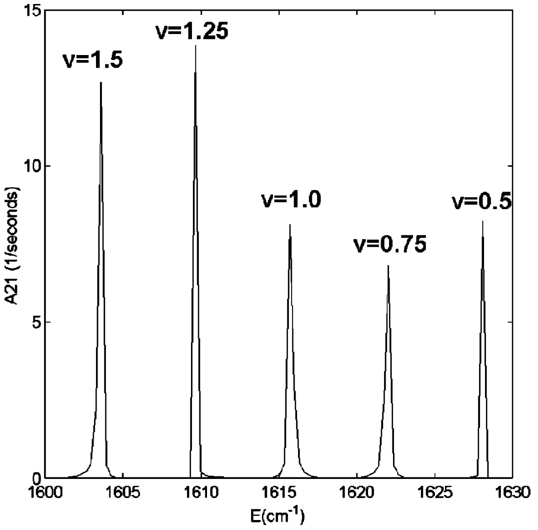

Figure 2. Classical collision spectra (CCS), $A_{\{u\}l}(\lambda)$, of CO computed with eq 6 over a limited spectral range, near $\Delta v = 1$ transitions. Five spectra are shown, each with a different classical action $l = (v, j)$: ($v = 0.5, j = 90$), ($v = 0.75, j = 90$), ($v = 1.0, j = 90$), ($v = 1.25, j = 90$), and ($v = 1.5, j = 90$).

with variations of the semiclassical action over a vibrational and rotational bin.

In quantum mechanics, spectra are usually generated by computing matrix elements between initial and final wave functions. For classical spectra, the optimal choice of semiclassical action is not immediately clear. As Noid et al. show, the best results are obtained by choosing a semiclassical action which is midway between the actions of the lower and upper states involved in the corresponding quantum transition.[1] This argument is motivated by examining the expression for the quantum mechanical spectral frequency. Following eqs 3.3−3.6 of ref 1 for a single mode, the quantum mechanical transition frequency is

$$\omega = E(n_f) - E(n_i) \cong (\partial E/\partial n)(n_f - n_i) \qquad (10)$$

where $E(n_f)$ and $E(n_i)$ are the final and initial energies of the transition, respectively, and the partial derivative, $\partial E/\partial n$ is evaluated at the mean value of the initial and final classical actions, $n = 1/2(n_f + n_i)$. Since the partial derivative of the energy with respect to the classical action is the classical frequency, the partial derivative, $\partial E/\partial n$, evaluated at the mean value of the actions is the usual classical mechanical angular frequency. Using the approximation of eq 10 therefore, we use trajectories evaluated at the mean actions of the transitions involved as best estimates for the corresponding quantum spectrum. For the present case of CO, these transitions correspond to the progression labeled ($v - 0.5, j = 89.5$), and give a nearly constant error with respect to the WKB energy of about -0.5 cm^{-1}. Varying the rotational action across a rotational bin, from $j = 89.0$ to $j = 90.0$, the energy error reaches about ±4 cm^{-1}. Varying the vibrational action across a vibrational bin from $n = v - 1$ to $n = v$ the energy error reaches about ±12 cm^{-1}. Investigations of several other transitions yield a similar result. Calculations with the "standard" numerical convergence parameters give nearly the same absolute errors in peak positions. This means that for transitions to the fundamental band, $\Delta v = 1$, there will be an inherent spread of the spectral peak positions of about 30 cm^{-1} with uniform (histogram)

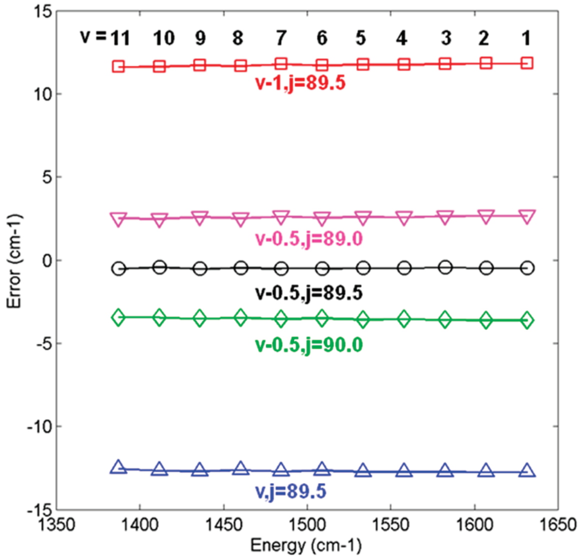

Figure 3. Energy versus error in CCS peak position with respect to WKB transition energies for 11 different transitions associated with the progression, $v, j = 90 \rightarrow v - 1, j = 89$, where $v = 1 \rightarrow 11$. CCS results are shown for five different choices of the semiclassical quantum numbers $l = (v, j)$: ($v - 0.5, j = 89.5$), ($v - 0.5, j = 90$), ($v - 0.5, j = 89$), ($v, j = 89.5$), and ($v - 1, j = 89.5$) with "fine" integration parameters.

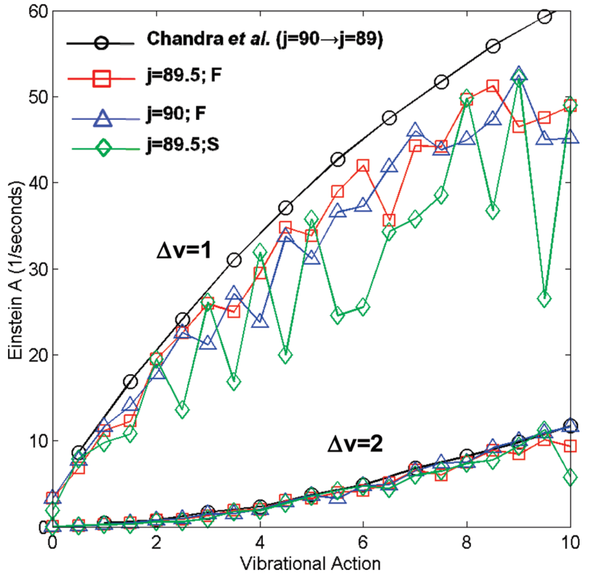

Figure 4. CCS Einstein *A* coefficients for fundamental ($\Delta v = 1$, $v \rightarrow v - 1$, $v = 1{-}9$, $j = 90 \rightarrow 89$) and overtone ($\Delta v = 2$, $v \rightarrow v - 2$, $v = 2{-}8$, $j = 90 \rightarrow 89$) progressions in CO as a function of the vibrational action. Results from three different CCS calculations are shown: (v, j = 89.5 (F)) the rotational action j = 89.5 with fine numerical convergence, (v, j = 90.0 (F)) j = 90.0 with fine numerical convergence, and (v = 89.5 (S)) j = 89.5 with standard numerical convergence. Einstein *A* values from Chandra et al.[23] are also plotted at the average vibrational action of the transition involved, $(v + (v - 1))/2$ for the fundamental and $(v + (v - 2))/2$ for the overtone.

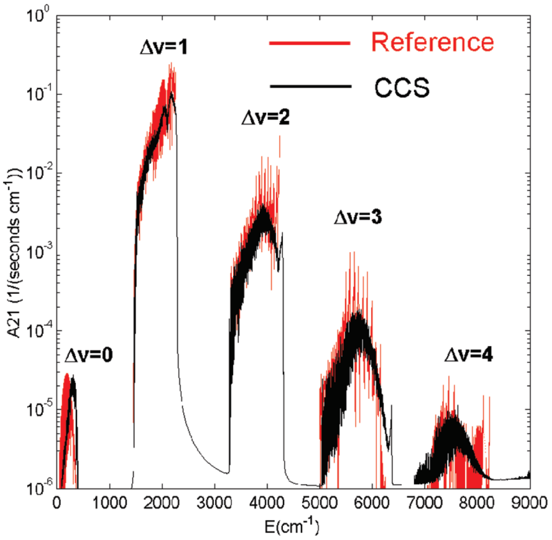

Figure 5. CCS per energy for collisions of O + CO at 8 km/s. Averaged CCS calculated from eq 7 with "standard" integration parameters using a weight of one for each trajectory (CCS). Also shown are results from eq 9, "reference", where the probabilities P_l are obtained from standard histogram binning into CO(v,j) states, the Einstein $A_{\{u\}l}$ are taken from Chandra et al.,[23] and the peak positions are taken from the WKB energies of individual (v, j) lines.

trajectory weighting, which although not very large, may wash out some of the expected structure in the collision averaged CCS of eq 7. Furthermore, for the first overtone band, we can expect the energy error spread to be larger, as trajectories with vibrational actions from $v = 0$ to $v = 2$ for example (centered around $v = 1$), will all contribute to the $v = 0 \rightarrow v = 2$ peaks.

To investigate the accuracy of the CCS peak heights, Figure 4 shows the CCS Einstein *A* coefficients for fundamental ($\Delta v = 1$, $v \rightarrow v - 1$, $v = 1{-}9$, $j = 90 \rightarrow 89$) and overtone ($\Delta v = 2$, $v \rightarrow v - 2$, $v = 2{-}8$, $j = 90 \rightarrow 89$) progressions in CO as a function of the vibrational action. Results from three different CCS calculations are shown: the rotational action $j = 89.5$ with fine numerical convergence, $j = 90.0$ with fine numerical convergence, and $j = 89.5$ with standard numerical convergence. We also show the computed Einstein *A* results of Chandra et al.[23] obtained with a different, but comparable CO potential and dipole moment function for a point of comparison. The Chandra et al. results are plotted at the average quantum number of the transition involved, $(v + (v - 1))/2$ for the fundamental and $(v + (v - 2))/2$ for the overtone, to more clearly illustrate the trends. It is well-known that Einstein *A* values, especially for higher vibrational states, are highly dependent on the fine details of the potential and dipole moment function. However, the Chandra et al. results will be a useful guide to the basic accuracy of the CCS peak heights and will indicate the degree accuracy expected of the CCS when highly accurate but not "exact" potentials and dipole moment functions are used. Except for the largest vibrational levels, the CCS fine integration results with $j = 89.5$ agree qualitatively with the results of Chandra et al. when the vibrational actions are equal to the average values of the transitions. This agrees with the work of Noid et al. and is consistent with the analysis of the energy values in Figures 2 and 3. Values of the Einstein *A* coefficients change smoothly with vibrational action. The relative change in the Einstein *A* values with vibrational action bracketing a particular transition, however, is much larger than the corresponding energy values. For example, for the fundamental transitions, the CCS Einstein *A* values change by a factor of ∼4 going from a vibrational action of 0 to 1, with the value at vibrational action of $^{1}/_{2}$ agreeing best with the Chandra et al. value. There is a much smaller sensitivity of the Einstein *A* to the rotational action. The integration error going from standard to fine convergence is surprisingly large for the fundamental band, especially for higher vibrational levels. For the overtone progression, we observe all the same trends, except that the differences between the Chandra et al. and CCS results are much less, and the integration errors are far less. The improved $\Delta v = 2$ integration errors may arise from the fact that important contributions to the spectrum could be coming from near the classical turning points, where the velocity is slower and the time-step requirements less severe. The better agreement with the results of Chandra et al. could likewise arise from better agreement between the present CO potential used here and that used by Chandra et al. near the classical turning points.

B. Averaged Trajectories. We now present results for the averaged CCS, eq 7. We will examine the collision system O + CO at 8 km/s and use the product CO position and momenta from previous QCT calculations.[12,13] A large spread of product CO vibrational and rotational states are accessed (v = 10+ and j = 100+), so this collision system makes for a good test case. Figure 5 shows averaged CCS calculated with "standard" integration parameters over a large scale, with a weight of one for each trajectory. The spectrum labeled "Reference" is used for comparison. This "Reference" spectrum is computed from eq 9, where the probabilities P_l are obtained from standard histogram binning into CO(v,j) states, the Einstein $A_{\{u\}l}$ are taken from Chandra et al.,[23] and the peak positions are taken from the WKB energies of individual (v, j) lines. The averaged CCS results have been divided by the energy bin width of 0.318 cm^{-1} and the eq 9 reference spectral peaks have been summed into 2.5 cm^{-1} bins to give common units of 1/(s cm^{-1}) to facilitate comparisons. We also note that both the averaged CCS results and the reference spectrum contain contributions from each

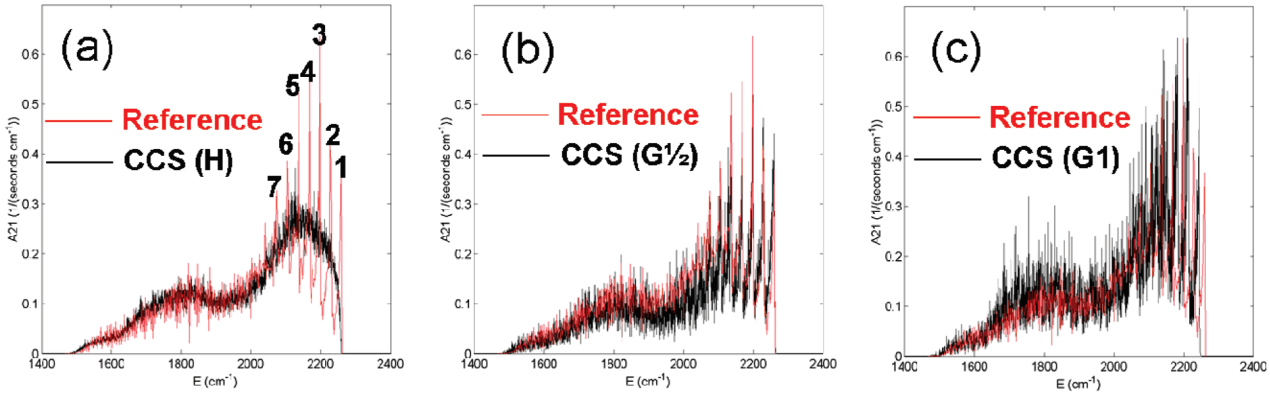

Figure 6. Same as Figure 5 in the fundamental band transition region with various trajectory weights used for the averaged CCS. H denotes standard histogram binning, with a weight of 1.0 for each trajectory and only vibrational actions with $v \geq 0.5$ are included, G(1/2) uses Gaussian weighting of trajectories centered on half-integer vibrational actions starting with $v = 0$, and G(1) uses Gaussian weights centered on integer vibrational actions starting at $v = 0.5$. For the reference spectrum only vibrational bins with $v > 0$ are included.

of the three lowest triplet electronic states involved in the O + CO collision system. For the averaged CCS, 1.e5 trajectories were averaged over for each electronic state, while the reference spectrum contained 2.5e5 trajectories to compute the QCT probabilities. In both spectra, most of the spectral intensity is due to "absorption" spectra of CO(v=0,j) product states (vibrationally elastic collisions), but the higher CO vibrational states also contribute significantly. The averaged CCS reproduces the overall intensities and extent of the different vibrational bands semiquantitatively. We do not expect exact agreement, as the Einstein *A* coefficients of the reference spectrum were obtained with a different potential and dipole moment function. However, there are some systematic differences which are due to the nature of the CCS. The averaged CCS is missing the band head structure due to high rotational state transitions evident in the $\Delta v = 2$ and $\Delta v = 3$ part of the reference spectrum. This is due to the spread of vibrational and rotational actions in each band, which shifts the position and modulates the strength of the CCS spectral lines. The shift and modulation of individual spectral lines tends to wash out any structure within a band. We have noted that as more trajectories contribute to the averaged CCS, the very fine structure evident in the $\Delta v = 4$ manifold tends to wash out, as in the $\Delta v = 1$ band. The averaged CCS also contains structure extending past the high energy part of the reference spectrum in each Δv region. This is due to the contributions from the large number of collisions which end up with vibrational actions near and below 0 (vibrationally elastic collisions). For these collisions the transition energies will tend to be overestimated, and this will give a spurious blue edged contribution to each Δv progression. We also note that as the number of averaged trajectories becomes greater and the sampling of vibrational and rotational actions becomes more continuous, the fine structure in each Δv progression begins to smooth away. This is due to modulation of peak positions and peak heights with the vibrational and rotational action of each single CCS trajectory contributing to the average.

We now investigate how choices of trajectory weights can bring out interesting structure in the averaged CCS and diminish some of the differences with the reference spectrum. We introduce a Gaussian weighting function of the form,[18,19,24]

$$G(v,s) = \frac{\beta}{\sqrt{\pi}} \exp(-(\beta(\mathrm{mod}(v+s,1.0)))^2) \qquad (11)$$

where v is the vibrational action. In eq 11, s can take on two values: either 1.0, which more heavily weights vibrational actions near integer values (G1 weighting), or 1.5, which more heavily weights half-integer values of the vibrational action (G1/2 weighting). The value of β is the bin-width parameter. Following previous experience,[24] we used a value of $\beta = 16.651$ which corresponds to a full-width-half-maximum (fwhm) of 0.1 across a vibrational action bin-width of 1.0. Figure 6 shows a close-up of the $\Delta v = 1$ fundamental region of the averaged CCS spectra using various trajectory weights. We also show the reference spectra where we have removed the vibrationally elastic ($v = 0$) contributions to the sum of eq 9 and instead of P_l we use P_u so the most blue transition (l → u) is 0→1, rather than $v = 1 \rightarrow 2$. Removing the dominant $v = 0$ contributions and plotting the reference spectrum in this way brings out the band head structure of the very high CO rotational states excited in the collision, which are labeled by their upper vibrational state. There are three average CCS results using different kinds of weights. Figure 6a shows the results including all vibrational actions greater than $v = 0.5$ and with weights of 1.0 for each trajectory, which we call histogram binning (H). Figure 6b shows the averaged CCS using Gaussian half-integer (G1/2) binning, according to eq 10, where only trajectories with vibrational actions greater than $v = 0.0$ are kept. Figure 6c shows Gaussian integer binning (G1), where only trajectories with vibrational actions greater than $v = 0.5$ are kept. The histogram binned results recover the extent, general shape, and magnitude of the reference spectra well. However, the histogram binned results wash out the band head peaks. This is due to the modulation of the peak height and position with the vibrational and rotational action which are equally weighted across bins. For the Gaussian half-integer weighted results, the band head structure is recovered well. For the fundamental band, the half-integer action weighting reduces the range of the vibrational action to regions near the half-integer values, which are optimal for the $\Delta v = 1$ fundamental band. The Gaussian integer weighted results recover the band-hand structure, but they are shifted too low in energy. The lowest vibrational actions (highest energy fundamental transitions) for the Gaussian integer results are centered near $v = 1$, which is optimal for $v = 0.5 \rightarrow v = 1.5$ transition and is shifted too low in energy for the $0 \rightarrow 1$ reference peak.

Figure 7a–c shows the same reference spectrum and average CCS results, but in the spectral range of the first overtone, $\Delta v = 2$. As in the previous figure, the (a)–(c) results show histogram, Gaussian half-integer, and Gaussian integer weight-

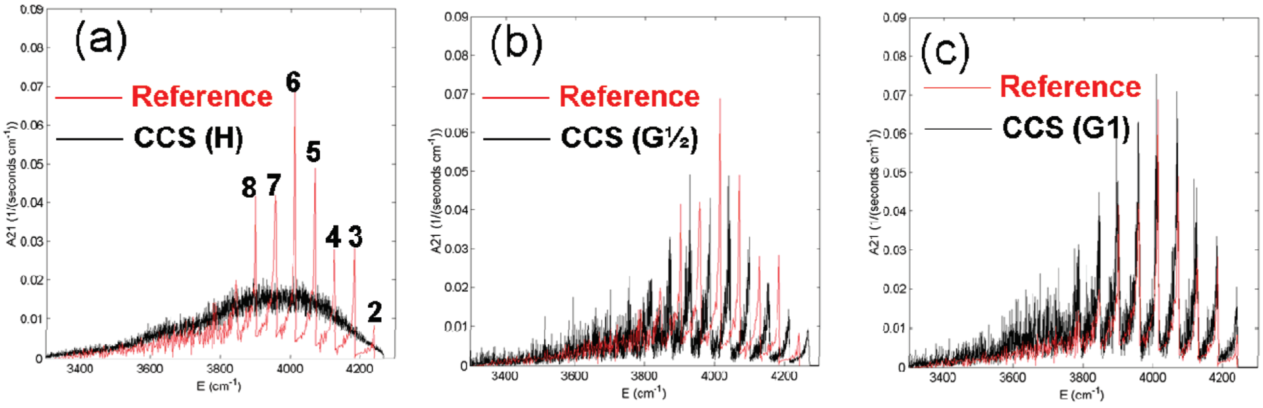

Figure 7. Same as Figure 6, except in the overtone region.

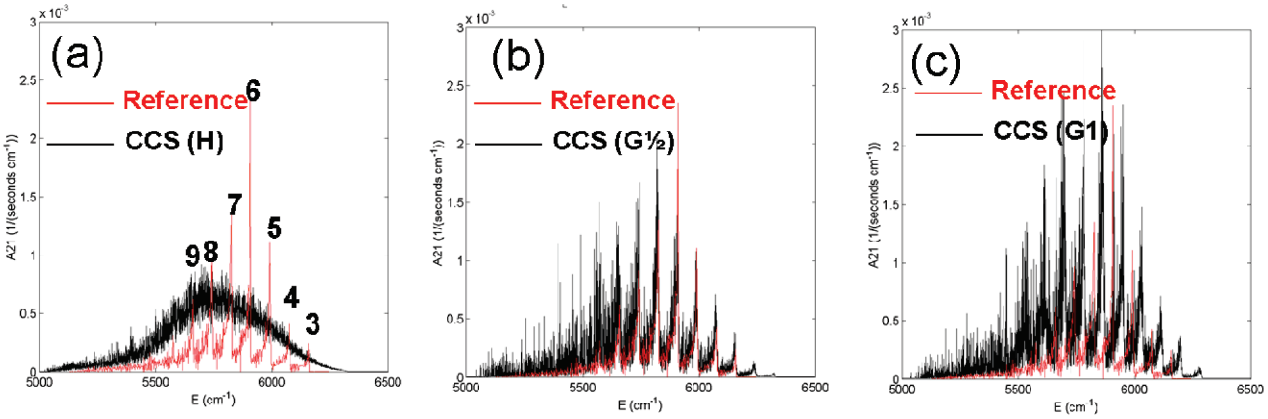

Figure 8. Same as Figure 6, except in the second overtone region.

ing, respectively. For the first overtone region, the Gaussian integer weighted results have the best match to the reference spectrum, reproducing the band head structure of the reference spectrum in detail. For the overtone reference spectra, the highest energy transitions are 0 → 2, and the averaged CCS centered on integer vibrational actions of 1 and higher, as is the Gaussian integer results, are optimal. Figure 8a–c shows the same reference and weighted results, but in the second overtone region, $\Delta v = 3$. Here the half-integer weighted results appear to match the reference spectra best. However, we note that at the high energy end of the spectrum, the average CCS extends past the reference spectrum. This is because the highest energy band head corresponds to 0 → 3 transitions, which corresponds to an optimal vibrational action of 1.5. Our half-integer Gaussian weighted average, however, starts with vibrational actions centered at 0.5, giving transition energies that are too large.

From the very good agreement between the CCS and reference spectra in Figures 6b and 7c with standard integration parameters, we expect that the semiclassical sources of error, which tend to shift the spectra systematically, will be a larger consideration than numerical error in practice.

IV. Conclusions

In this paper, we formulated an extension of the work of Noid et al.[1] to obtain classical spectra through Fourier transform of the dipole moment function of collision product trajectories. We showed that this "classical collision spectrum" (CCS) is related to a set of Einstein *A* values and transition energies. We then showed that a weighted average CCS, obtained in the usual way from standard QCT Monte Carlo trajectory methods, is related to a sum of ro-vibrational specific cross sections times a set of Einstein *A* values. As a test case we computed the CCS of single trajectories of CO. We investigated the sensitivity of the CCS to numerical convergence parameters and the dependence of the CCS on the vibrational and rotational actions. We then applied the method to generating averaged CCS from O + CO collisions at 8 km/s. The averaged CCS of these trajectories shows rich quantum-like structure including well-separated vibrational overtones and rotational band heads, which becomes more pronounced with particular trajectory weighting methods.

The computation of average CCS is a straightforward extension of existing classical trajectory methods. Future work will apply the classical spectral methods developed here to collisions of polyatomic systems and analysis of polyatomic products. Using direct dynamics methods, which should yield forces and dipole moment functions at each trajectory point, it should be possible to calculate the average CCS straightforwardly, even for large molecular systems. With knowledge of the Einstein *A* coefficients of collision products, in principle it should be possible to deconvolve the average CCS and estimate probabilities to quantum specific final states. The hope is that the contributions from various vibrational modes will separate more cleanly in the classical spectra than in conventional QCT energy binning methods. Finally we note that the CCS should be directly comparable to the absorption spectrum of nascent collision products in molecular beam experiments, and so may provide a useful common point of comparison between theory and measurements.

For polyatomic systems, an important possible complication of the present analysis is that the products may undergo internal relaxation or some other process during the time period of the

Fourier transform. Furthermore, chaotic trajectories may introduce a dense forest of spectral lines within vibrational bands and effectively broaden spectral features. Classically chaotic motion, some of which may not have a quantum analog, may introduce spurious structure into the CCS. At higher energies, where classically chaotic motion is more likely, spectral broadening will make it more difficult to extract quantum specific cross sections.

However, for the system examined here and for many other polyatomic systems[11] chaotic trajectories may not be a real difficulty in practice. High resolution of spectral features may not be required in many applications, where for example it is sufficient to separate bending and stretching vibrational motions. Furthermore, to the extent that the collision products are quasi-periodic, spectral estimation methods, such as linear prediction and filter diagonalization, can be used to decrease trajectory times and increase computational efficiency. One benchmark polyatomic application we plan on pursuing in the near future is the collisional excitation of H_2O by fast O-atoms, where interesting data[25,26] and new potential surfaces[27] exist. In this case, exact quantum scattering treatments are possible, so that classical and quantum-mechanical ro-vibrationally specific cross sections can be compared using the same surface. O-atom interactions with hydrocarbon systems are also of current interest[28] and could be examined in future work.

Acknowledgment. We acknowledge support through a Small Business Innovative Research (SBIR) award, contract number W9113M-07-C-0152, Dr. Marty Venner, technical monitor. We also acknowledge several helpful technical discussions with R. Dressler, L. Bernstein, and H. Dothe of Spectral Sciences, Inc.

References and Notes

(1) Noid, D. W.; Koszykowski, M. L.; Marcus, R. A. *J. Chem. Phys.* **1977**, *67*, 404.

(2) Brown, A.; Braams, B. J.; Christoffel, K.; Jin, Z.; Bowman, J. M. *J. Chem. Phys.* **2003**, *119*, 8790.

(3) Kim, J.; Schmitt, U. W.; Gruetzmacher, J. A.; Voth, G. A.; Scherer, N. E. *J. Chem. Phys.* **2002**, *116*, 737.

(4) Schatz, G. C. *Comput. Phys. Commun.* **1988**, *51*, 135.

(5) Nizamov, B.; Setser, D. W.; Wang, H.; Peslherbe, G. H.; Hase, W. L. *J. Chem. Phys.* **1996**, *105*, 9897.

(6) Truhlar, D. G.; Muckerman, J. T. Reactive Scattering Cross Sections III: Quasiclassical and semiclassical methods. In *Atom Molecule Collision Theory*; Bernstein, R. B., Ed.; Plenum: New York, 1979.

(7) Noid, D. W.; Koszykowski., M. L.; Marcus, R. A. *Annu. Rev. Phys. Chem.* **1981**, *32*, 267.

(8) Sewell, T. D.; Thompson, D. L.; Gezelter, J. D.; Miller, W. H. *Chem. Phys. Lett.* **1992**, *193*, 512.

(9) Swamy, K. N.; Hase, W. L. *Chem. Phys. Lett.* **1982**, *92*, 371.

(10) Cho, Y. J.; Winter, P. R.; Harris, H. H.; Fleischmann, E. D.; Adams, J. E. *J. Phys. Chem.* **2002**, *94*, 1847.

(11) Sewell, T. D.; Thompson, D. L.; Levine, R. D. *J. Phys. Chem.* **1992**, *96*, 8006.

(12) Braunstein, M.; Duff, J. W. *J. Chem. Phys.* **2000**, *112*, 2736.

(13) Brunsvold, A. L.; Upadhyaya, H. P.; Zhang, J.; Cooper, R.; Minton, T. K.; Braunstein, M.; Duff, J. W. *J. Phys. Chem. A* **2008**, *112*, 2192.

(14) Upschulte, B. L.; Caledonia, G. E. *J. Chem. Phys.* **1992**, *96*, 2025.

(15) Green, B. D.; Holtzclaw, K. W.; Joshi, P. B.; Burke, H. K. *J. Geophys. Res.-Space Phys.* **1992**, *97*, 12161.

(16) McQuarrie, D. A. *Statistical Mechanics*; Harper Row: New York, 1976.

(17) Penner, S. S. *Quantitative Molecular Spectroscopy and Gas Emissivities*; Addison-Wesley: Reading, MA, 1959.

(18) Bonnet, L. R.; Rayez, J.-C. *Chem. Phys. Lett.* **1997**, *227*, 183.

(19) Bonnet, L. R.; Rayez, J.-C. *Chem. Phys. Lett.* **2004**, *397*, 106.

(20) Banares, L.; Aoiz, F. J.; Honvault, P.; Bussery-Honvault, B.; Launay, J.-M. *J. Chem. Phys.* **2003**, *118*, 565.

(21) Langhoff, S. R.; Bauschlicher, C. W., Jr. *J. Chem. Phys.* **1995**, *102*, 5220.

(22) Allen, M. P.; Tildesley, D. J. *Computer Simulation of Liquids*; Clarendon Press: Oxford, U.K., 1987.

(23) Chandra, S.; Maheshwari, V. U.; Sharma, A. K. *Astron. Astrophys. Suppl. Ser.* **1996**, *117*, 557.

(24) Xie, T.; Bowman, J.; Duff, J. W.; Braunstein, M.; Ramachandran, B. *J. Chem. Phys.* **2005**, *122*, 014301.

(25) Meyerott, R. E.; Swenson, G. R.; Schweitzer, E. L.; Koch, D. G. *J. Geophys. Res.* **1994**, *99*, 17.

(26) Bernstein, L. S.; Elgin, J. B.; Pike, C. P.; Knecht, D. J.; Murad, E. E.; Zehnpfennig, T. F.; Galicia, G. E.; Stair, A. T. *J.Geophys.Res.* **1996**, 383.

(27) Braunstein, M.; Panfili, R.; Shroll, R.; Bernstein, L. *J. Chem. Phys.* **2005**, *122*, 184307.

(28) Yan, T.; Doubleday, C.; Hase, W. L. *J. Phys. Chem. A* **2004**, *109*, 9863.

JP904055Y